

MODELLING OF SOOT PARTICLE COLLISION AND GROWTH PATHS IN GAS-SOLID TWO-PHASE FLOW

by

Hongling JU^{a,b}, Fanquan BIAN^b, and Mingrui WEI^{a,b*}

^aHubei Key Laboratory of Advanced Technology for Automotive Component,
Wuhan University of Technology, Wuhan, China

^bHubei Collaborative Innovation Center for Automotive Components Technology,
Wuhan University of Technology, Wuhan, China

Original scientific paper
<https://doi.org/10.2298/TSCI191110215J>

Particle collision is an important process in soot particle growth. In this research, based on gas-solid two-phase flow, particle trajectory was traced by the Lagrange approach with periodic boundaries. Trajectory intersection, collision probability, and critical velocity were considered, and the growth path of each particle was traced. The collision frequency, f_c , agglomeration frequency, f_a , and friction collision frequency, f_{cf} , were calculated, and the main influence factors of particle collision were analyzed. The results showed that f_c , f_a , f_{cf} increased with the increase of the particle volume fraction and gas phase velocity, v , but the particle initial diameter, d_{pi} , and velocity had the great influence on f_{cf} . f_{cf} obviously decreased with the increase of d_{pi} and v . The statistical analysis of f_{cf} and Stokes number showed that f_{cf} decreased with the increase of Stokes number, especially when Stokes number was extremely small, f_{cf} decreased rapidly. Using the trajectory analysis of each particle, the particle growth process could be classified in three types: firstly, the particles that did not agglomerate with any particles during the entire calculation process, secondly, the particles that continually agglomerated with small particles to generate larger ones, and finally, the particles that were agglomerated by larger particles at some calculation moment.

Key words: gas-solid flow, Lagrange approach, particle size distribution, agglomeration, friction collision, particle growth path

Introduction

Particulate matter pollution is one of the most serious atmospheric environmental problems, and it has attracted increasing attention in the world. The fine particles produced by fuel combustion are usually called soot particles.

The growth process of soot particles is usually divided into two-stages: the gas-phase chemical reaction and particle dynamics [1, 2]. Under the action of the gas-phase chemical reaction, soot particles nucleate. The gas-phase chemical reaction includes fuel pyrolysis, growth species (C_2H_2) formation, polycyclic aromatic hydrocarbons formation, and nucleation [3]. In a combustion device, the growth of soot nuclei is a complex multi-phase flow process; that is, the gas (continuous phase) and soot nuclei (discrete phase) are mixed by extremely complex and transient turbulent motion. Therefore, non-linear, non-equilibrium, non-uniform, and multi-scale couplings exist between the discrete and continuous phases and between the discrete and

* Corresponding author, e-mail: weimingrui@whut.edu.cn

discrete phases, that makes the complex dynamics evolution process of soot nuclei growing into soot particle is inevitable. This process mainly includes dynamic events such as collision, agglomeration, surface deposition, breakage and surface chemical reaction, *etc.* Researchers have done a large amount of research on these dynamic events. Mohaghegh *et al.* [4] modeled the collisions of arbitrary-shaped particles. Stubing *et al.* [5] studied particle agglomeration and the fluid dynamic behavior of agglomerates. Yu *et al.* [6] direct numerical simulated polydisperse aerosol particle deposition in low Reynolds number turbulent flow. Karimi and Andersson [7] conducted an exploratory study on fluid particle breakup rate models. The aforementioned studies only focus on a single dynamic event, but the dynamic evolution process of soot particles is the result of the combined effects of dynamic events.

Under the joint action of dynamic events, the sizes of soot particles increase from the nanometer level to the micron level, and undergo changes in a nuclear state, an aggregation state, and a coarse state [8]. In these dynamic events, collision and agglomeration were considered as the main factors to affect size distribution and morphology of soot particles [9].

Collision and agglomeration are usually considered in both semi-empirical and detailed soot models, such as the Kazakov-Foster semi-empirical soot model [10], the phenomenological soot modelling approach of Zhao *et al.* [2], and the Frenklach-Maus detailed soot model [11], *etc.* These soot models usually use an overall reaction describe a collision and agglomeration process, and different numerical methods are used to calculate the reaction rate of the collision and agglomeration process. One method is the Arrhenius equation, which is used to calculate the collision rate [2, 10]. Other methods include the method of moments [11, 12] and the Monte-Carlo method [13], which are used to calculate particle group balance equations. The aforementioned methods can calculate the mass and size of soot particles, but the calculated particle size is nanometer level [2, 11], which is less than the experimental measurement value [14]. This shows that the overall reaction of collision and agglomeration cannot fully reflect the dynamic evolution process of soot particles growth.

Because soot particles randomly move in turbulence for an engine cylinder, soot particles are discrete phase, and whose trajectory is one of criterions whether collision occurs. Collide may occur when the trajectories of the two particles simultaneously cross. The calculation method of particles trajectories in the air-flow can be divided into two categories: the Lagrange method and the Euler method. The Lagrange method takes the particles as the description object and tracks the trajectory and velocity of every particle [15, 16], but it is heavy computation burden. The Euler method takes the spatial position as the description object and records the velocity of the particle that occupies a specific spatial position at a specific time [17]. This method has a small amount of computation, but can't track the trajectory of every particle.

Except the trajectories of particles, a collision needs the collision kernel model. The physical meaning of the collision kernel model is the rate of collisions within the computational domain of the discrete system. Saffman *et al.* [18] first put forward a collision sphere-based accurate geometric collision-kernel, β , model of zero inertial particles. The β is average collision kernel, and it can be used to calculate collision number, N , per unit time in a unit volume, $N = \beta n_i n_j$, n_i and n_j are number density of particle groups i and j , respectively. On this basis, the collision kernel β formulas were proposed based on the cylindrical mode and the spherical mode, respectively [18]. Park *et al.* [19] adopted the formula based on the spherical mode to simulate particle collision under high Reynolds number flows. Sommerfeld [20], in contrast, introduced the formula based on cylindrical mode to simulate particle collision and agglomeration in turbulent flows.

In addition the equations based on the cylindrical mode and the sphere mode, the Smoluchowski collision rate coefficient can be used to describe the stochastic collision of particles in the collision kernel model [15, 21]. In calculation of the model, the kinematic simulation method [22] and direct numerical simulation method [23] are used to calculate collision frequency of particles that reflects the probability of particle collision. According to the aforementioned methods, the collision frequency can be calculated in turbulent, shear, or laminar flow. The particles studied in the previous methods are round particles, but the shape of the practical particles is irregular. Currently, studies on collision of elliptical particles [24] and collision of irregular particles [4] have also been conducted.

In conclusion, the aforementioned methods are based on the random principle for studying the collision frequency between particles. Most of the current dynamic events can calculate the possibility of the occurrence of dynamics events in gas-solid two-phase flow, and they can summarize the particle size distribution, but it is difficult to track the growth process of every particle.

In this work, based on the gas-solid two-phase flow, particle trajectory is traced by using Lagrange method with periodic boundaries. Trajectory intersection, collision probability, and critical velocity are considered in order to calculate the collision frequency, f_c , agglomeration frequency, f_a , and friction collision frequency, f_{fc} , in a computational domain. The effects of particles initial diameters, d_{pi} , particles number, N_{pi} , gas phase temperature, t , and gas phase velocity, v , on the particle collision, agglomeration, and friction collision are analyzed, and the growth process of each particle in the computational domain is summarized. The calculation flow chart used in this work is shown in fig. 1.

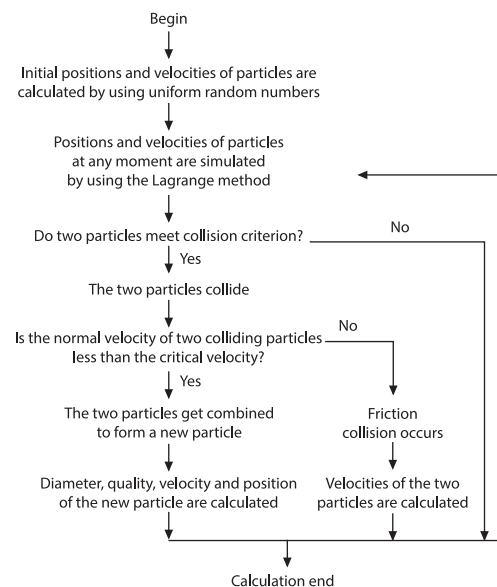


Figure 1. Calculation flowchart of particle collision

Particle collision dynamics event

In this paper, two changes are made based on model of Ho and Sommerfeld [15], including: trajectories intersection added in the collision criterion of two particles and the transformation between the rectangular co-ordinate system and the $u-v$ collision co-ordinate system, and a revised collision model is established. The revised collision model can be used to calculate f_c , f_a , and f_{fc} , and to track the movement trajectory of each particle in a computational domain. Here are two changes in the revised collision model as follow.

Collision and agglomeration criterion of two particles

According to kinetic theory, the occurrence of a collision is decided based on collision probability, P_c , [15]. The P_c stands for the collision possibility between any two particles in the computing domain. Because only two particles in contact may collide, particles trajectory intersections are considered in this work. Therefore, trajectory intersections and P_c are used to determine whether particles collide, and the collision criterion of two particles is calculated:

$$P_c = \frac{\pi}{4} (d_{p1} + d_{p2})^2 |\vec{V}_1 - \vec{V}_2| N_p \Delta t, \quad RN < P_c, \quad D \leq \frac{d_{p1} + d_{p2}}{2} \quad (1)$$

where P_c is calculated by considering the relative velocities $|\vec{V}_1 - \vec{V}_2|$ of the colliding particles, d_{p1} and d_{p2} are the particle diameters, N_p – the number of particles in computational domain, RN – the uniform random number in range $[0,1]$, and D – the distance between the center of two particles.

When two particles satisfy the collision criterion, the particles collide. Once particles collide, an agglomeration or a friction collision may occur. The critical velocity, v_{cr} , determines whether two particles will agglomerate or not. The v_{cr} is calculated [15]:

$$v_{cr} = \frac{1}{d_p} \frac{(1-e^2)^{1/2}}{e^2} \frac{A}{\pi z_0^2 \sqrt{6 p_{pl} \rho_p}} \quad (2)$$

where e is the coefficient of restitution, A – the Hamerker constant, z_0 – the contact distance, P_{pl} is the material limiting contact pressure, d_p – the average diameter of all the particles in the computational domain, and ρ_p – the particle density. The agglomeration of particles will occur when the following condition is satisfied:

$$|\vec{u}_1 - \vec{u}_2| \cos \phi \leq v_{cr} \quad (3)$$

where \vec{u} is the normal velocity of the particle.

When particles agglomerate, the parameters of the new particle need to be calculated, including the mass, diameter, velocity, energy, etc. Otherwise, the two particles have a friction collision that is an inelastic collision [25], in which the masses and sizes of the two particles remain constant, but the velocities and energies of the two particles change.

The transformation of the co-ordinate system during a friction collision

In the gas-solid two-phase flow, a particle has both radial velocity and circumferential velocity, as shown in fig. 2, \vec{V}_i is radial velocity, Ω – circumferential velocity [25]. When two particles occur a friction collision, a co-ordinate system is established, as shown in fig. 2. The u -axis passes through the center of the two particles, the v -axis lies in the plane established by the u -axis and the relative velocity vector of the two particles, and the velocity in the w -direction is zero. Therefore, the friction collision between two particles is a 2-D collision in the u - v

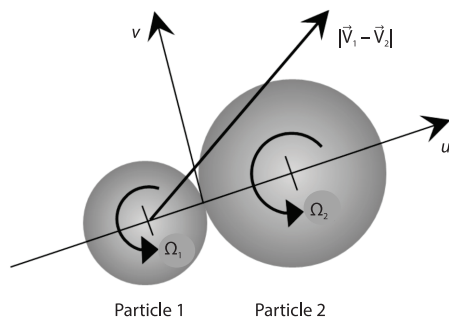


Figure 2. The u - v co-ordinate system for the friction collision of two particles

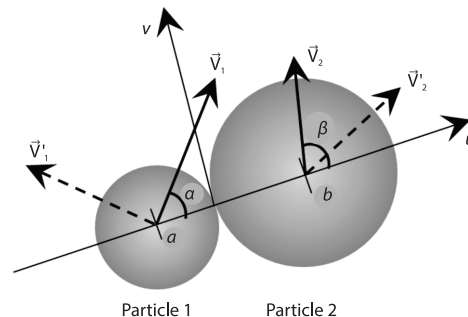


Figure 3. Schematic diagram of velocity vectors before and after friction collision in the new u - v co-ordinate system

co-ordinate system. The u is the normal velocity component and the v is the transverse velocity component. Because the computational domain is in the rectangular co-ordinate system and the particles trajectories need to be tracked, the normal and transverse velocities in the u - v co-ordinate system and the velocity components in the rectangular co-ordinate system need to be transformed. Figure 3 shows the velocity vector before and after the friction collision of two particles in a u - v co-ordinate system.

In fig. 3, \vec{V}_1 and \vec{V}_2 are the velocity vectors of Particle 1 and Particle 2 before a friction collision, respectively. The \vec{V}'_1 and \vec{V}'_2 are the velocity vectors of Particle 1 and Particle 2 after a friction collision, respectively. Before a friction collision, the angle between the u -axis and the velocity vector of Particle 1 is denoted by α , and the angle between u -axis and the velocity vector of Particle 2 is denoted by β . The normal and transverse velocities in the u - v co-ordinate system before the friction collision are calculated with the dot product:

$$u_{p1} = |\vec{V}_1| \cos \alpha, \quad v_{p1} = |\vec{V}_1| \sin \alpha, \quad u_{p2} = |\vec{V}_2| \cos \beta, \quad v_{p2} = |\vec{V}_2| \sin \beta \quad (4)$$

The circumferential velocity is ignored, and the normal velocities of the two particles after the friction collision can be obtained with momentum conservation and Coulomb's law of friction [15]:

$$u'_{p1} = u_{p1} \left(1 - \frac{1+e}{1+m_{p1}/m_{p2}} \right) \quad (5)$$

$$u'_{p2} = \frac{m_{p1}(u_{p1} - u'_{p1}) + m_{p2}u_{p2}}{m_{p2}} \quad (6)$$

where m_{p1} and m_{p2} are the masses of Particles 1 and 2, respectively.

Considering whether there is slip between Particles at the moment of collision, according to Coulomb's law of friction, the condition for no slip between particles [15]:

$$\frac{u_{p1}}{v_{p1}} < \frac{7\mu_f(1+e)}{2} \quad (7)$$

where μ_f is the coefficient of friction.

The transverse velocity component for a non-sliding collision:

$$v'_{p1} = v_{p1} \left(1 - \frac{2}{7} \right) \quad (8)$$

The transverse velocity component for a sliding collision:

$$v'_{p1} = v_{p1} \left[1 - \mu_f(1+e) \frac{u_{p1}}{v_{p1}} \frac{1}{1+m_{p1}/m_{p2}} \right] \quad (9)$$

According to momentum conservation, the transverse velocity of Particle 2 is calculated:

$$v'_{p2} = \frac{m_{p1}(v_{p1} - v'_{p1}) + m_{p2}v_{p2}}{m_{p2}} \quad (10)$$

The velocities of two particles after a friction collision can be calculated:

$$|\vec{V}'_1| = \sqrt{u'^2_{p1} + v'^2_{p1}}, \quad |\vec{V}'_2| = \sqrt{u'^2_{p2} + v'^2_{p2}} \quad (11)$$

The velocity component vectors of Particles 1 and 2 after a friction collision in the rectangular co-ordinate system can be calculated with the dot product. These values are the velocity condition of the next moment.

Initial conditions

Particle collision is an inevitable part of the particle growth process in turbulence. The effects of the particle initial parameters (d_{pi} , N_{pi} , etc.) and fluid parameters (t , v , etc.) on particle growth are studied in a fixed hexahedron computational domain. The calculation domain ($0.1 \text{ cm} \times 0.1 \text{ cm} \times 0.1 \text{ cm}$) is a microvolume in the circular tube with a diameter of 0.12 m, and the turbulence in that is assumed as uniform and isotropic. Turbulent kinetic energy and turbulence dissipation rate are calculated according to the references [26]. The periodic boundary is used in the calculation. The initial conditions are listed in tab. 1.

Table 1. Calculation initial conditions

Parameters	Value	Parameters	Value
Particles number	10^4 - 10^5	Gas phase velocity	0.15-3 m/s
Particles initial diameters	2-9 μm	Reynolds number	2300 - $4.7 \cdot 10^4$
Particles density	2.25 g/cm^3	Turbulent kinetic energy	1.2-240 m^2/s^2
Particles volume fraction	$2 \cdot 10^{-4}$ - $2 \cdot 10^{-2}$	Turbulent dissipation rate	0.5-700 m^2/s^3
Gas phase temperature	20-500 $^\circ\text{C}$	Time step	$5.0 \cdot 10^{-6}$ s
Hydraulic diameter	0.12 m	The end time	$5.0 \cdot 10^{-4}$ s

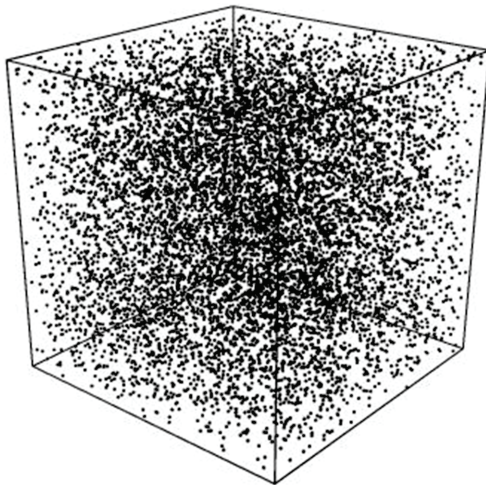


Figure 4. Initial distribution diagram of 10000 particles with a diameter of 5 μm in the computational domain

In the calculation domain, the initial position of each particle is equal to the uniform random number in the range $[0, 1]$ times the length of the computational domain. Figure 4 shows that an initial distribution of 10000 particles with a diameter of 5 μm in the computational domain. This indicates that the particles are uniformly distributed in the calculation domain. All the initial particles are spherical in the calculation.

Effects of the particle initial parameters on collisions

Figure 5 shows the effects of d_{pi} and N_{pi} on f_c , f_a , f_{fc} and f_a/f_c when t is 20 $^\circ\text{C}$ and v is 2 m/s. The f_a/f_c refers to the ratio of the agglomeration frequency to the collision frequency. Because the result of collision of two particles may be agglomeration or friction collision, f_a/f_c

can indicate the proportion of agglomeration in all particles collisions under every calculation condition.

According to eq. (1), when the initial velocity of the particles is constant, P_c and the particle volume fraction (the ratio of the particle total volume to the volume of the computational domain) increase with the increase of d_{pi} . This indicates that free space of particles decreased

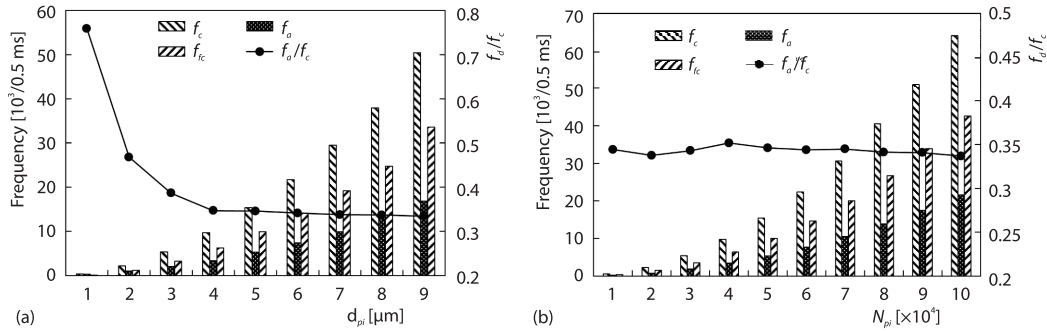


Figure 5. Effects of d_{pi} and N_{pi} on f_c , f_a , f_{fc} , f_a/f_c when t is 20°C and v is 2 m/s; (a) d_{pi} and (b) N_{pi}

in the computational domain. Therefore, the probability of the particle trajectory intersections increases. That is, f_c , f_a , and f_{fc} increase with the increase of d_{pi} . However, f_a/f_c decreases with the increase of d_{pi} , this is because that the larger the particle diameter is, the smaller v_{cr} is, and lead to the lower f_a , see eq. (3).

In order to ensure that particles have enough space in the computational domain, the particle volume fractions are roughly within the range of $2 \cdot 10^{-4}$ - $2 \cdot 10^{-2}$ in this work. When d_{pi} is $5 \mu\text{m}$, the effects of N_{pi} on particle collision are studied. As can be seen from fig. 5(b), f_c , f_a , and f_{fc} increase with the increase of N_{pi} , but f_a/f_c basically remains unchanged. This is because that the increasing number of particles, the volume fraction of such particles in the computational domain also increases, which directly decreases the free-activity room, so f_c , f_a , and f_{fc} increase. However, d_{pi} , v , and t are unchanged at different N_{pi} , so v_{cr} and Stokes number are unchanged, which leads to f_a/f_c little difference.

Figure 6 shows the particle size distribution for different N_{pi} at $5.0 \cdot 10^{-4}$ s. As can be seen from fig. 6, because f_a increases with the increase of N_{pi} , the particle size distribution range becomes larger from $[5, 7.22] \mu\text{m}$ to $[5, 12.4] \mu\text{m}$. After agglomeration, the number of small-sized particles decreases, while the number of large-sized particles increases. Therefore, the larger the particle number is, the larger f_a is, and the larger the particle size distribution range is.

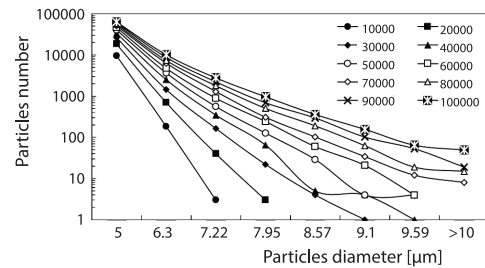


Figure 6. Particles size distribution for different N_{pi} after $5.0 \cdot 10^{-4}$ s (d_{pi} is $5 \mu\text{m}$, v is 2 m/s, and t is 20°C)

Effects of fluid parameters on collisions

Figure 7 shows the effects of v and t on f_c , f_a , f_{fc} , and f_a/f_c when d_{pi} is $5 \mu\text{m}$ and N_{pi} is 50000, respectively. As can be seen from fig. 7(a), f_c , f_a , and f_{fc} increase with the increase of v , but f_a/f_c decreases. When Hydraulic diameter and t remain unchanged, Reynolds number increases from $2.34 \cdot 10^3$ to $4.69 \cdot 10^4$ with the increase of v , turbulence is more intense, and velocities of particles are bigger to increase f_c , f_a , and f_{fc} . The velocities increase of particles makes the relative velocity of the two colliding particles even greater. Meantime, v_{cr} is same at different v because d_{pi} remains unchanged. By comparing eq. (3), it can be seen that it is more difficult to meet the conditions of agglomeration with the increase of v , therefore, f_a/f_c decreases.

When d_{pi} is $5 \mu\text{m}$, N_{pi} is 50000 and v is 2 m/s, t has almost no effects on collisions, as shown in fig. 7(b). The t rises, the gas kinematic viscosity increases and density decreases. According to Reynolds number equation, Reynolds number decreases with the increase of t . Al-

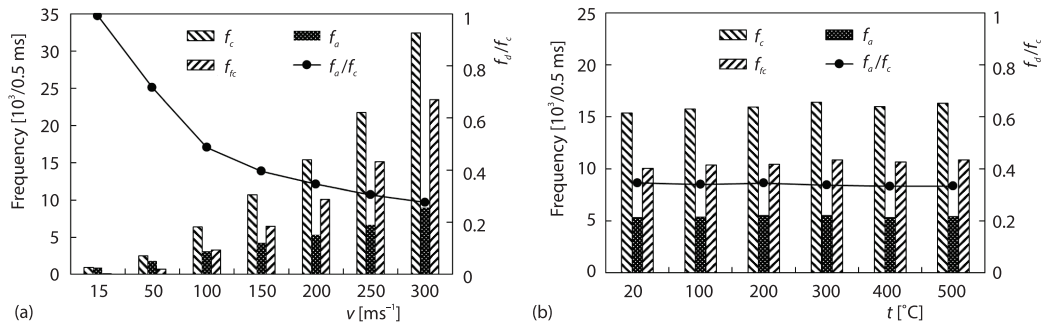


Figure 7. Effects of v and t on f_c , f_a , f_{fc} , and f_d/f_c when d_{pi} is $5 \mu\text{m}$ and N_{pi} is 50000; (a) v and (b) t

though Reynolds number decreases, but v remains unchanged, the accelerating action of solid phase by gas phase remains unchanged, so f_c , f_a , and f_{fc} have a little change. This makes f_d/f_c basically unchanged.

Due to f_a increases with the increase of v , the number of bigger-particles increases, while the number of smaller-particles decreases. The particle size distribution range increases from $[5, 8.57] \mu\text{m}$ to $[5, 12.4] \mu\text{m}$, as shown in fig. 8(a). However, the particle size distribution rang has little different at different t because t has almost no effects on collisions, and the particle size distribution range is $[5, 10] \mu\text{m}$, as shown in fig. 8(b). Based on figs. 7 and 8, it can be seen that gas phase velocity has a greater influence on particle collision and agglomeration because of the accelerating action of particles by gas phase.

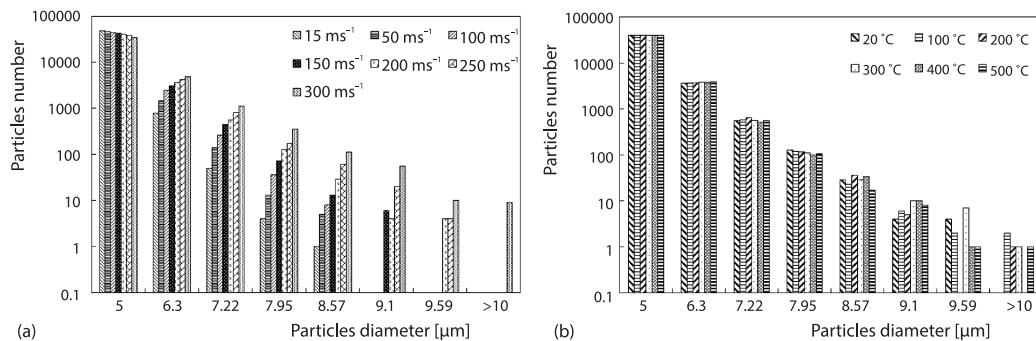


Figure 8. Particles size distribution for different v and t after $5 \cdot 10^{-4} \text{ s}$ when d_{pi} is $5 \mu\text{m}$ and N_{pi} is 50000

The particles in gas-solid flow can be divided into three categories by the Stokes number: fine particle, finite-inertial particle, and coarse particle [27]. The Stokes number is calculated using the following equation [27]:

$$Stk = \frac{\rho_p d_p^2}{18 \rho_f \left[\left(\frac{v^3}{\varepsilon} \right)^{1/4} \right]^2} \quad (12)$$

where ρ_p and ρ_f are the density of the particles and the density of the air, respectively, and v – the kinematic viscosity.

According to eq. (12), the Stokes number increases from $3.21 \cdot 10^{-4}$ to $3.12 \cdot 10^{-2}$. This indicates that the collision of the finite inertial particles is studied in this work. Figure 9 marks Stokes numbers and f_d/f_c at different conditions, and fits a curve. It can be seen that the smaller Stokes number is, and the bigger f_d/f_c is. When Stokes numbers are smaller than 0.005, f_d/f_c decreases rapidly. But when Stokes numbers are bigger than 0.005, f_d/f_c decreases slowly. This is because that Stokes number represents the followability of particles in the flow. The smaller the Stokes number of the particles is, the stronger the ability of the particles to follow the fluid becomes [15]. Therefore, in particles collisions, the probability of agglomeration is greater, that is, f_d/f_c is bigger.

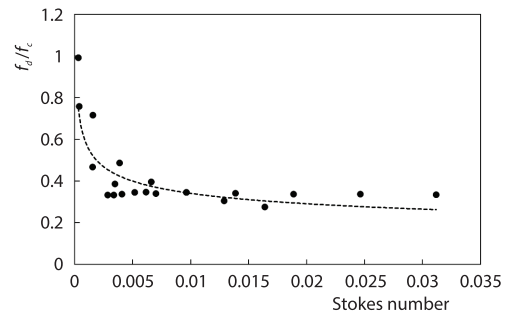


Figure 9. The change of f_d/f_c with Stokes number

Growth processes of particles

Soot particles grow and change due to different dynamics events in gas-solid flow. When d_{pi} is 5 μm , v is 2 m/s, and N_{pi} is 50000, the particles size distribution range is [5, 9.59] μm . The particles growth paths can be divided into three groups in the computational domain: firstly, the particles do not agglomerate with any particles during the entire calculation process, secondly, the particles continually agglomerate with small-sized particles to generate larger ones, finally, the particles are agglomerated by larger particles at some calculation moment.

The 21151th particle is the largest particle at the end of calculation. The 21151th particle agglomerates the other six particles to form a large particle with a diameter of 9.56 μm . Figure 10(a) shows the initial distribution of the seven initial particles at the begin of calculation. In order to show the relative position of the particles more clearly, the region where the particles are located is enlarged, as shown in fig. 10(b).

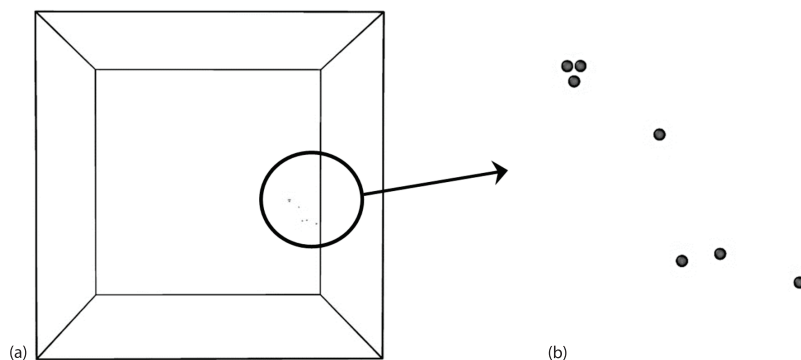


Figure 10. The initial distribution of the 21151th particles and the other 6 initial particles agglomerated by the 21151th particles

In order to show the growth process of the 21151th particles, an region of 0.03×0.035 cm is intercepted in the left view of the computational domain. The 21151th particle occurs six times agglomeration with the 6046th, the 33766th, the 49832th, the 18726th, the 42225th, and the 12574th particles, respectively, and finally forms the biggest polymer at $3.1 \cdot 10^{-4}$ s, as shown in fig. 11. Until the end of the calculation, no agglomeration occurs.

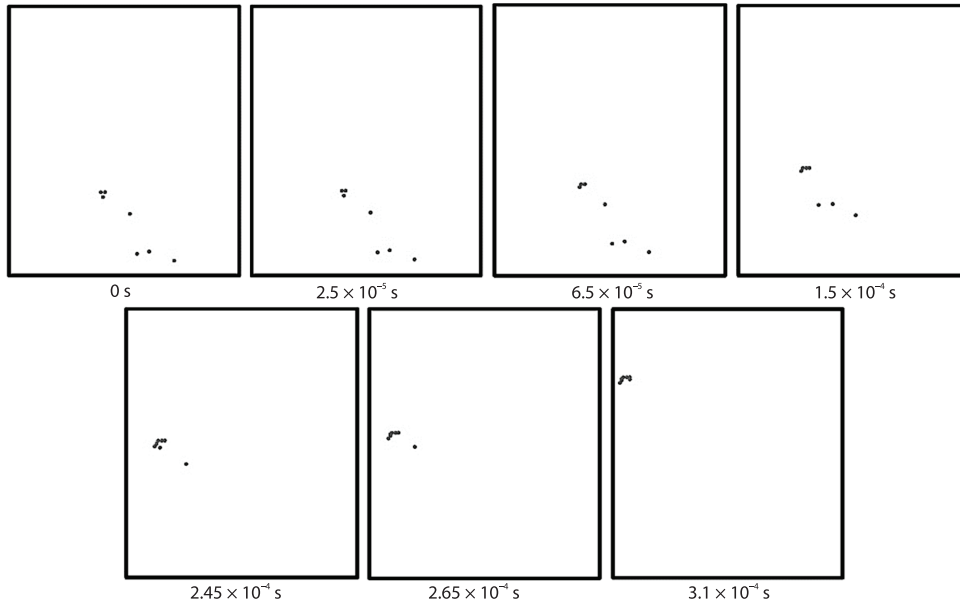


Figure 11. The growth progress of the 21151th particle; (a) 0 s, (b) $2.5 \cdot 10^{-5}$ s, (c) $6.5 \cdot 10^{-5}$ s, (d) $1.5 \cdot 10^{-4}$ s, (e) $2.45 \cdot 10^{-4}$ s, (f) $2.65 \cdot 10^{-4}$ s, and (g) $3.1 \cdot 10^{-4}$ s

Conclusions

Based on the gas-solid two-phase flow, the particle trajectory was traced using the Lagrange approach with periodic boundaries. The trajectory intersection, collision probability, and critical velocity were considered, and the growth path of each particle could be traced. The main factors affecting particle collision were analyzed, and the growth paths of the particles were summarized. The force of particles was not considered in the complete calculation. The specific conclusions are given.

- With the particles volume fraction increased, f_c , f_a , and f_{fc} increased, however, d_{pi} had a greater influence on f_a/f_c , and f_a/f_c decreased with the increase of d_{pi} .
- Compared with t , v had a greater impact on particle collisions. With v increased, f_c , f_a , f_{fc} and size distribution range increased, but f_a/f_c decreased.
- The f_a/f_c had a great relationship with the Stokes number. The smaller the Stokes number was, the larger the f_a/f_c was. On the contrary, the larger the Stokes number was, the f_a/f_c decreased slowly.
- The growth paths of the particles were summarized in the computational domain. Firstly, the particles did not agglomerate with any particles during the entire calculation process. Secondly, the particles continually agglomerated with small-sized particles to generate larger ones. Finally, the particles were agglomerated by larger particles at some calculation moment.

Acknowledgment

This study was funded by the National Science Foundation for Young Scientists of China (Grant No. 51706163) and Wuhan University of Technology.

References

- [1] Tao, F., *et al.*, A Phenomenological Model for the Prediction of Soot Formation in Diesel Spray Combustion, *Combustion and Flame*, 136 (2004), 3, pp. 270-282
- [2] Zhao, F., *et al.*, Numerical Modelling of Soot Formation and Oxidation Using Phenomenological Soot Modelling Approach in a Dual-Fueled Compression Ignition Engine, *Fuel*, 188 (2017), Jan., pp. 382-389
- [3] Zhou, D. Z., *et al.*, An Enhanced Primary Reference Fuel Mechanism Considering Conventional Fuel Chemistry in Engine Simulation, *Journal Engineering for Gas Turbines and Power*, 138 (2016), Sept., No. 092804-1-8
- [4] Mohaghegh, F., Udaykumar, H. S., Modelling Collisions of Arbitrary-Shaped Particles in Simulations of Particulate Flows, *Powder Technology*, 344 (2019), Feb., pp. 756-772
- [5] Stubing, S., *et al.*, Modelling Agglomeration and the Fluid Dynamic Behavior of Agglomerates, Report No. AJK2011-12025, *Proceedings*, ASME-JSME 2011, Joint Fluids Engineering Conference, Hamamatsu, Japan, 2011
- [6] Yu, L., *et al.*, Direct Numerical Simulation of Polydisperse Aerosol Particles Deposition in Low Reynolds Number Turbulent Flow, *Annals of Nuclear Energy*, 121 (2018), Nov., pp. 223-231
- [7] Karimi, M., Andersson, R., An Exploratory Study on Fluid Particles Breakup Rate Models for the Entire Spectrum of Turbulent Energy, *Chemical Engineering Science*, 192 (2018), Dec., pp. 850-863
- [8] Kittelson, D., *et al.*, Review of Diesel Particulate Matter Sampling Methods, Final Report University of Minnesota, Minneapolis, Minn., USA, 1999
- [9] Wang, L., *et al.*, Numerical Simulation of the Growth of Nanoparticles in a Flame CVD Process, *China Particuology*, 2 (2004), 5, pp. 215-221
- [10] Kazakov, A., Foster, D. E., Modelling of Soot Formation during DI Diesel Combustion Using a Multi-Step Phenomenological Model, SAE Paper, No. 982463, 1998
- [11] Frenklach, M., Wang, H., Detailed Modelling of Soot Particle Nucleation and Growth, *Proceedings of the Combustion Institute*, 23 (1991), 1, pp. 1559-1566
- [12] Shao, T., *et al.*, Effect of Soot Model, Moment Method, and Chemical Kinetics on Soot Formation in a Model Aircraft Combustor, *Proceeding of the Combustion Institute*, 37 (2019), 1, pp. 1065-1074
- [13] Yan, B., Caffisch, R. E., A Monte-Carlo Method with Negative Particles for Coulomb Collisions, *Journal of Computational Physics*, 298 (2015), Oct., pp. 711-740
- [14] Xiao, H., *et al.*, An Experimental Study of the Combustion and Emission Performances of 2,5-dimethylfuran Diesel Blends on a Diesel Engine, *Thermal Science*, 21 (2017), 1B, pp. 543-553
- [15] Ho, C. A., Sommerfeld, M., Modelling of Micro-Particle Agglomeration in Turbulent Flows, *Chemical Engineering Science*, 57 (2002), 15, pp. 3073-3084
- [16] Lain, S., Sommerfeld, M., Characterization of Pneumatic Conveying Systems Using the Euler/Lagrange Approach, *Powder Technology*, 235 (2013), Feb., pp. 764-782
- [17] Ray, M., *et al.*, An Euler-Euler Model for Mono-dispersed Gas-particle Flows Incorporating Electrostatic Charging Due to Particle-Wall and Particle-Particle Collision, *Chemical Engineering Science*, 197 (2019), Apr., pp. 327-344
- [18] Saffman, P. G., Turner, J. S., On the Collision of Drops in Turbulent Clouds, *Journal of Fluid Mechanics*, (1956), 1, pp. 16-30
- [19] Park, K. S., Heister, S. D., Modelling Particle Collision Processes in High Reynolds Number Flow, *Journal of Aerosol Science*, 66 (2013), Dec., pp. 123-138
- [20] Sommerfeld, M., Validation of a Stochastic Lagrangian Modelling Approach for Inter-Particle Collision in Homogeneous Isotropic Turbulence, *International Journal of Multi-phase Flow*, 27 (2001), 10, pp. 1829-1858
- [21] Jorge, H. O., On the Diffusion- Controlled Rate Coefficient for Chemical Reactions and Collisions of Nano Particles, *Chemical Engineering Science*, 171 (2017), Nov., pp. 481-484
- [22] Meyer, D. W., Eggersdorfer, M. L., Simulating Particle Collisions in Homogeneous Turbulence with Kinematic Simulation – A Validation Study, *Colloids and Surfaces A: Physicochemical and Engineering Aspects*, 454 (2014), July, pp. 57-64
- [23] Gui, N., *et al.*, Numerical Study of Particle-Particle Collision in Swirling Jets: A DEM-DNS Coupling Simulation, *Chemical Engineering Science*, 65 (2010), 10, pp. 3268-3278
- [24] Saini, N., Kleinstreuer, C., A New Collision Model for Ellipsoidal Particles in Shear Flow, *Journal of Computational Physics*, 376 (2019), Jan., pp. 1028-1050
- [25] Oesterle, B., Petitjean, A Simulation of Particle-to-Particle Interaction in Gas-solid Flow, *International Journal of Multi-Phase Flow*, 19 (1993), 1, pp. 199-211

- [26] ***, Ansys, Inc., Ansys Fluent User's Guide, <http://www.ansys.com>
- [27] Alipchenkov, V. M., Zaichik, L. I., Particle Collision Rate in Turbulent Flow, *Fluid Dynamics*, 36 (2001), 4, pp. 608-618